

ERASMUS MUNDUS MASTERS IN COMPLEX SYSTEMS

**DYNAMICS OF RANDOMLY
CONNECTED SYSTEMS WITH
APPLICATIONS TO NEURAL NETWORKS**

July 9, 2012

L. C. García del Molino
École Polytechnique
garciadelmolino@paris-diderot.fr

Supervisors:

Prof. Khashayar PAKDAMAN, Institut Jacques Monod, Paris
Prof. Jonathan TOUBOUL, Collège de France, Paris

Intro for the layman

Write some stuff here

Abstract

In this report I analyze the behavior of a randomly connected system of non-linear neuron analog elements. I complement the existing literature regarding homogeneous networks by studying finite size effects. I also describe the behavior of heterogeneous networks. Perform linear stability analysis. I propose mean field model

Contents

1	Introduction	5
2	Model	5
3	Numerical exploration	7
3.1	Homogeneous network	7
3.2	Heterogeneous network, non balanced coupling	8
3.3	Heterogeneous network, balanced coupling	9
4	Heuristics	9
5	Linear stability analysis	10
5.1	Infinite systems	11
5.2	Finite systems	12
6	Mean field equations	14
7	Conclusions	14
A	Numerical simulation details	16
B	Optimal system size for spontaneous activity	16
C	Proof of the global asymptotic stability of 0 for $\sigma < 1$ in the homogeneous network in the limit $N \rightarrow \infty$	17
D	Derivation of the mean field equations	18

1 Introduction

A key feature of complex systems is that they exhibit a high variability in their microscopic characteristics. Very often this variability is averaged resulting in regular macroscopic behaviors. This does not mean however that macroscopic properties can be easily deduced from the microscopic description. In fact building the mathematical link between the micro and macro scales requires sophisticated techniques and careful analysis.

In the field of network theory and its applications to neurosciences, variability has often been modeled as the existence or lack of edges between two nodes. In such cases the adjacency matrix provides a full description of the network. However in [1] they show that the behavior of certain neural networks strongly depends on the synaptic weights. This means that in order to make an accurate description of a neural network one should consider not only which pairs of nodes are connected but also what is the intensity of each connection.

Variability in the intensity of connections has generally been implemented through random matrices. The idea was popularized in [2] with applications to ecological networks and soon after that an application to neural networks appeared in [3]. The main tools used to understand such systems from a mathematical point of view have been mean field techniques and linear stability analysis for which many results coming from random matrix theory are needed.

The aim of this project is to understand rigorously the role of variability within the synaptic weights in a firing rate neural network model starting from the model used in [3,4]. Some effort has been devoted to extend the results of the existing literature, however the main goal of the project has been to describe and understand the behavior of the model after including a physiologically relevant feature: the distinction between excitatory and inhibitory neurons.

The report is structured as follows: in Section 2, I introduce the model presenting briefly the state of the art and raising the main questions that are to be answered. In Section 3, I show the observations resulting from numerical simulations of the system under different conditions and parameter values. These simulations are focused on the time evolution of the system and they recall the questions raised in the previous section. In the rest of the report I try to shed some light upon the underlying phenomena that give rise to the observed behavior using different independent approaches. Section 4 contains an heuristic analysis of the main equations that, far from being mathematically rigorous, should provide some intuitive ideas about the behavior of the model. In Section 5, I review the linear stability analysis that can be found in the literature and apply it to our system. I also present a new theorem regarding the spectral properties of random matrices and apply it to the model. Finally in Section 6, I propose a system of mean field equations and sketch how will they be analyzed in a future work.

2 Model

We consider a network consisting of $N_E = fN$ excitatory neurons and $N_I = (1-f)N$ inhibitory neurons. The state of the network is given by the value of the membrane potentials $\{x_i\}_{i=1,\dots,N}$ whose dynamics obey

$$\dot{x}_i = -x_i + \sum_j w_{ij} S(x_j) . \quad (2.1)$$

The first term on the right hand side accounts for the tendency of the neurons to equilibrate their inner potential with that of the environment and prevents the system from diverging. The the second term contains the input that the i th neuron receives from the rest of the network. The input coming from the j th neuron is a centered sigmoid of x_j with slope 1 at the origin and is proportional to the synaptic weight $w_{ij} = \frac{1}{\sqrt{N}} (\mu M_{ij} + \sigma J_{ij})$.

$$M_{ij} = \begin{cases} \sqrt{\frac{1-f}{f}} & \text{for } j < fN \\ -\sqrt{\frac{f}{1-f}} & \text{for } j \geq fN \end{cases}$$

is the deterministic part of the coupling and establishes the category, either excitatory or inhibitory, of neuron j . Notice that since the category of the j th neuron is independent on the neuron receiving the input all rows in M are identical. Furthermore the elements of M are chosen such that each row sums up to 0. Whenever M appears with only one subindex I will be referring to the vector containing one row of M . On the other hand J is a random matrix whose elements are drawn from a distribution such that

$$\begin{aligned} \mathbb{E}[J_{ij}] &= 0 \\ \mathbb{E}[J_{ij}J_{kl}] &= \delta_{ik}\delta_{jl} . \end{aligned}$$

J is introduced to model the random variability in the synaptic weights. Note that J is quenched: it is drawn once and fixed forever therefore the dynamics of the system are deterministic. This is an important difference with respect to many other models where the variability is introduced through Wiener processes and hence the dynamics are stochastic. I will pay special attention to networks with balanced coupling, that is $\sum_j w_{ij} = 0$. Since M_{ij} is balanced by definition, in order to have balanced coupling one has to impose $\sum_j J_{ij} = 0$. Because the matrices that satisfy the previous condition are a zero-measure subset of the set containing all matrices J I will use the special notation \bar{J} for balanced matrices. Note that while J can be both balanced or non balanced results for J hold almost surely and may not be true for \bar{J} . $w = (w_{ij})_{1 \leq i, j \leq N}$ is the connectivity matrix. The scaling $\frac{1}{\sqrt{N}}$ is set such that in the limit of large networks the input term $\sum_j w_{ij} S(x_j)$ remains $\mathcal{O}(1)$.

It is convenient to express the variables x_i as a sum of the population average and a “difference” term. Denoting $\langle x \rangle = \frac{1}{N} \sum_i x_i$ one has

$$x_i = \langle x \rangle + y_i .$$

Then it is possible to rewrite (2.1) as a system of $N+1$ equations (one for the average and N for the difference terms) with the advantage that in the limit $N \rightarrow \infty$ the equations for the difference terms do not depend explicitly on the deterministic part of the coupling (μM) and the equation for the average does not depend explicitly on the random part of the coupling (σJ). The equation that governs the dynamics of $\langle x \rangle$ is found taking the average of (2.1)

$$\begin{aligned} \dot{\langle x \rangle} &= -\langle x \rangle + \sum_j \langle w_{ij} \rangle S(x_j) \\ &= -\langle x \rangle + \sum_j (\mu M_j + \sigma \langle J_{ij} \rangle) S(x_j) . \end{aligned} \tag{2.2}$$

The dynamics of the difference terms are given by

$$\begin{aligned} \dot{y}_i &= \dot{x}_i - \langle \dot{x} \rangle = -y_i + \sum_j (w_{ij} - \langle w_{ij} \rangle) S(x_j) \\ &= -y_i + \sum_j \sigma (J_{ij} - \langle J_{ij} \rangle) S(x_j). \end{aligned} \quad (2.3)$$

Depending on the choice of the parameters the observed behavior changes qualitatively:

- $\mu > 0, \sigma = 0$: there is no disorder and the whole the system reduces to two equations whose analysis is trivial. The deterministic coupling is balanced and hence all membrane potentials decay exponentially to zero. In the steady state the network remains inactive.
- $\mu = 0, \sigma > 0$: the network is *homogeneous* in the sense that there is no differentiation between excitatory and inhibitory neurons. This model has been extensively studied for J non balanced in [3–6]. Mean field solutions and their stability are known. In the limit $N \rightarrow \infty$ there is a phase transition at $\sigma = 1$. For $\sigma < 1$ the trivial solution $x_i = 0$ for all i is globally asymptotically stable. For $\sigma > 1$ many attractors exist but the only stable one is chaos. On the other hand, according to heuristic results in [4], several stable attractors may co-exist in the region $\sigma \sim 1$ in finite systems. These are either non zero equilibrium points or limit cycles, and as σ is increased the limit cycles become more complex, eventually leading to chaotic attractors. The region where these new attractors exist starts close to the mean field phase transition and its width shrinks to zero as N is increased. There are no rigorous results regarding finite size effects, the phase transition at $\sigma = 1$ is not understood from the classical bifurcation theory point of view and it is not clear whether the known results hold for \bar{J} or not.
- $\mu > 0, \sigma > 0$: the network is *heterogeneous* since the outputs of excitatory and inhibitory neurons have different averages. The spectral properties of this model have been studied [7, 8]. There is no description or explanation for the global behavior which differs qualitatively from that of $\mu = 0$. Within this setup we study both the balanced and non balanced coupling scenarios.

3 Numerical exploration

The technical details about the simulations can be found in Appendix A.

3.1 Homogeneous network

Simulations confirm the finite size effects described in [4] (see Fig. 1). Furthermore one can see that there is a very big variability on the dynamics from one sample to another. Drawing different random matrices from the same distribution results in completely different outcomes among the possible behaviors (i.e. fixed points, limit cycles or chaotic trajectories). The length of the window in σ where finite size effects are observed also changes significantly from one realization to another. The average membrane potential fluctuates around 0 and the typical size of the

fluctuations seems to decrease as the system size is increased suggesting that they are finite size effects. As a side part of this project I have estimated the probability

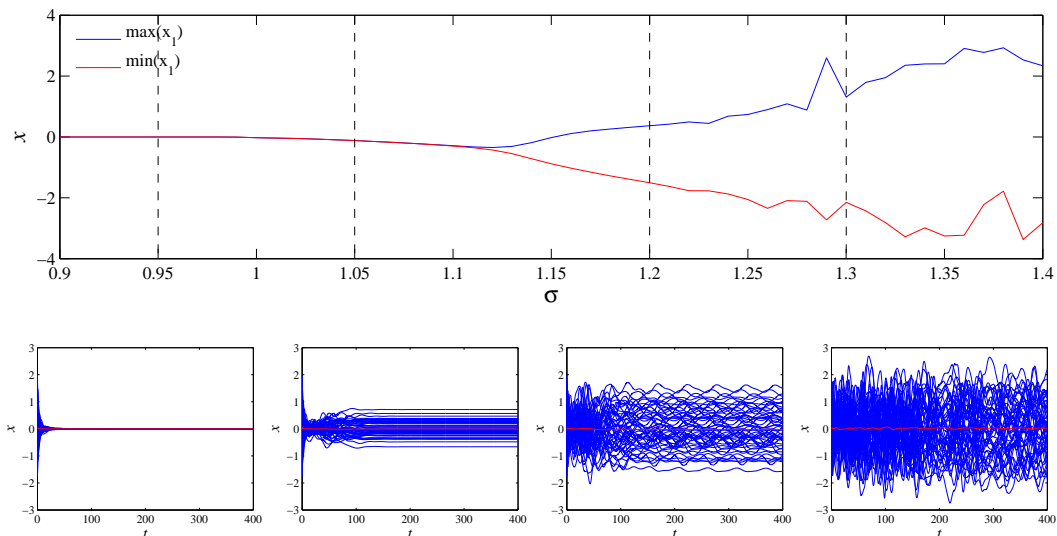


Figure 1: Simulations of the homogeneous model with $N = 1000$. **Top:** bifurcation diagram for one realization of J and one initial condition. The blue and red lines represent the maximum and minimum values of the membrane potential of one neuron over a time interval $t \in [200, 400]$, after the transitory regime. When the minimum and maximum have the same value the system has reached a fixed point. Otherwise the system oscillates. Regularity in the amplitude of the oscillations for changing σ suggests that the oscillations are limit cycles, while irregularity points to chaos. In the interval $\sigma \in (0.95, 1.4)$ there are a series of classical bifurcations (pitchfork and Hopf) before the chaos settles. **Bottom:** in red the average membrane potential of the network. In blue the trajectories of the individual membrane potentials $\{x_i\}_{1 \leq i \leq N}$ for different values of sigma. From left to right $\sigma = \{0.95, 1.05, 1.2, 1.3\}$ and the respective observed attractors are: fixed point at 0, fixed point other than 0, periodic oscillations, chaotic oscillations. In all cases the mean is very close to 0.

of observing spontaneous activity for $\sigma < 1$ as a function of N . Numerical results suggest that there is an optimal $N^*(\sigma)$ that maximizes this probability. Some details about the computations and the interpretation of the results can be found in the appendix B.

3.2 Heterogeneous network, non balanced coupling

The first remarkable numerical observation is that very often 0 loses its stability for $\sigma < 1$. The position of the first bifurcation, despite changing widely from one realization to another, does not seem to depend on the system size. The second observation is that in this case the mean has non trivial dynamics whose typical amplitude does not vary when the system size is modified. Fig. 2 shows a bifurcation diagram and some typical trajectories. Finally there is some synchronization among neurons in the sense that $\text{Var}[x_i]$ is small compared to the homogeneous model. One way to quantify synchronization is to compute the correlation coefficients between all pairs of neurons over a time interval and average them. Doing so for different realizations of the system and different values of the parameters one can estimate the expected degree of synchronization for a pair (σ, μ) . Results in Fig. 3 show that

this synchronization decreases with increasing system size so it might be a finite size effect.

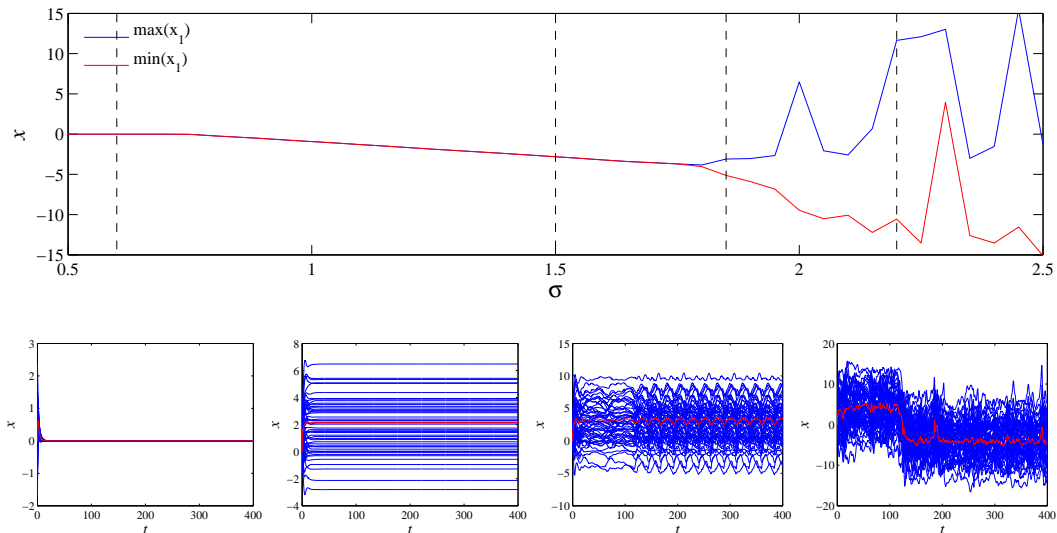


Figure 2: Simulations of the homogeneous model with $N = 1000$. **Top:** bifurcation diagram for one realization of J and one initial condition. The first transition takes place way before $\sigma = 1$. Eventually the trajectories become chaotic. **Bottom:** From left to right $\sigma = \{0.6, 1.5, 1.85, 2.2\}$ and the respective observed attractors are: fixed point at 0, fixed point other than 0, periodic oscillations, chaotic oscillations. Note that in this case the dynamics of the mean are not centered around 0.

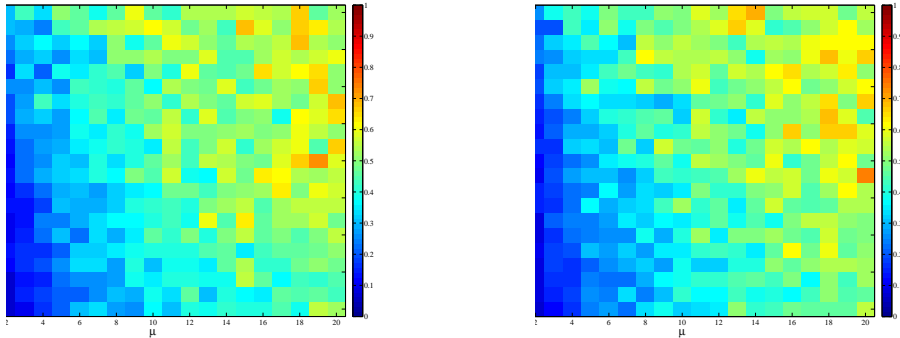
3.3 Heterogeneous network, balanced coupling

The heterogeneous balanced network is with no doubt the more interesting one from the phenomenology point of view. Typical trajectories for this system are shown in Fig. 4. The first observation is that again the average of the membrane potentials has nontrivial dynamics. Secondly it exhibits strong synchronization that does not disappear when the system size is increased. Also in some cases, specially when $\mu \gg \sigma$, there are relaxation oscillations. This last observation is specially striking since no new timescale has been introduced. In general increasing μ results in stronger synchronization and more regularity of the dynamics of the average.

4 Heuristics

A deeper look at the system consisting of equations (2.2) and (2.3) can provide useful hints. I will use the shorthand notation

$$\begin{aligned}
 A &= \sum_j (\mu M_j + \sigma \langle J_{ij} \rangle) S(x_j) , \\
 B_i &= \sum_j \sigma (J_{ij} - \langle J_{ij} \rangle) S(x_j) , \\
 \bar{B}_i &= \sum_j \sigma (\bar{J}_{ij} - \langle \bar{J}_{ij} \rangle) S(x_j) .
 \end{aligned} \tag{4.1}$$



(a) $N = 1000$

(b) $N = 2000$

Figure 3: Correlation coefficients averaged over 10 different initial conditions. The correlations decrease slightly when the system size is increased from $N = 1000$ to $N = 2000$.

As the rows of M and \bar{J} sum up to 0, $|A|$ and $|\bar{B}_i|$ will be small if $\text{Var}[S(\langle x \rangle + y_i)]$ is small. However for non balanced J , $|B_i|$ will be large except if all x_i are close to 0, which is very unlikely in the chaotic regime. To understand the behavior of $\text{Var}[S(\langle x \rangle + y_i)]$ it is important to remark that, due to the saturation of $S(x)$ when $|x| \rightarrow \infty$, if $|\langle x \rangle| \gg 1$ and $\text{Var}[y_i] \lesssim |\langle x \rangle|$ then $\text{Var}[S(\langle x \rangle + y_i)]$ is small. On the other hand, when $|\langle x \rangle| \ll 1$ and $\text{Var}[y_i]$ is large then $\text{Var}[S(\langle x \rangle + y_i)]$ is large. These relations are summarized in the following table

	$\text{Var}[y_i] \lesssim \langle x \rangle $	$\text{Var}[y_i] \gg \langle x \rangle $
$ \langle x \rangle \gg 1$	A and \bar{B}_i small	A and B_i large
$ \langle x \rangle \ll 1$	A and B_i small	A and B_i large

The first conclusion that can be drawn from this analysis regards the non zero dynamics of the mean when $\mu > 0$. In the homogeneous network model one has $\mu = 0$ and $\langle x \rangle$ decays exponentially to 0 up to fluctuations generated by $\langle J_{ij} \rangle$. By the central limit theorem $\langle J_{ij} \rangle = \mathcal{O}(1/\sqrt{N})$. This means that A can be made arbitrarily small by increasing the system size and the dynamics of the mean are finite size effects. When $\mu > 0$, A is $\mathcal{O}(1)$ and the dynamics of the mean do not disappear for increasing N .

The second conclusion is that the balance condition together with the saturation of $S(x)$ allow synchronization when $|\langle x \rangle|$ is large. Since the membrane potentials are not allowed to grow indefinitely it is unlikely that $\text{Var}[y_i] \gg |\langle x \rangle|$. Therefore $|\bar{B}_i|$ becomes small when $|\langle x \rangle|$ is large resulting in an exponential decay of y_i and consequently of $\text{Var}[x_i]$.

5 Linear stability analysis

Because 0 is always a solution of (2.1) it is reasonable to start by studying its stability. Linearization around 0 yields

$$\dot{x}_i = -x_i + \sum_j w_{ij} x_j \quad (5.1)$$

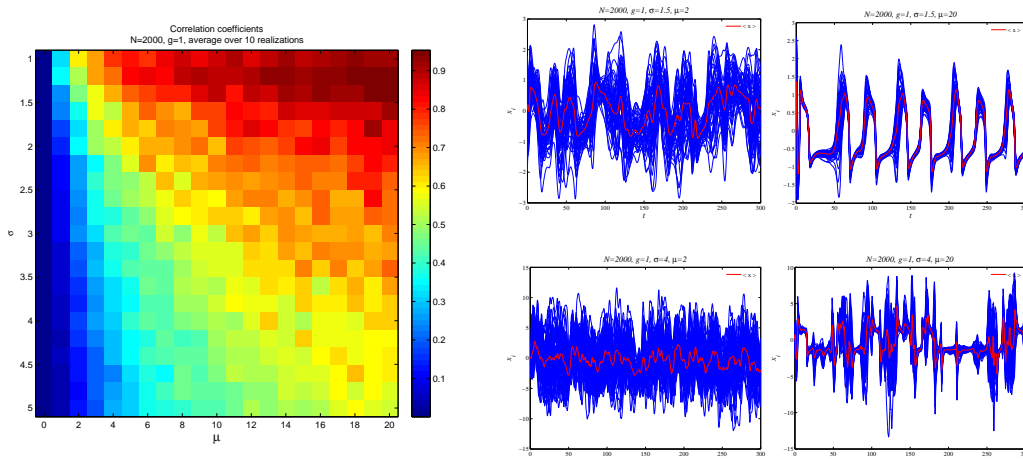


Figure 4: **Left:** Averaged correlation coefficients for 10 realizations of a system with $N = 2000$. **Right:** Trajectories for $N = 2000$. The values of the parameters from left to right and top to bottom are $\sigma = 1.5, \mu = 2$, $\sigma = 1.5, \mu = 20$, $\sigma = 4, \mu = 2$, $\sigma = 4, \mu = 20$.

and the stability of 0 will be given by the eigenvalue with maximal real part of $-I+w$. Computing the eigenvalues of such matrix requires results of random matrix theory. I first introduce some useful definitions:

Definition 5.1. An *iid random matrix* is an $N \times N$ matrix $J = (J_{ij})_{1 \leq i, j \leq N}$ whose entries J_{ij} are iid complex entries with $\mathbb{E}[J_{ij}] = 0$ and $\mathbb{E}[J_{ij}J_{kl}] = \delta_{ik}\delta_{jl}$.

Definition 5.2. Given an $N \times N$ complex matrix w , we define the *empirical spectral distribution* μ_w to be the probability measure

$$\mu_w := \frac{1}{N} \sum_i \delta_{\lambda_i}$$

where $\{\lambda_i\}_{1 \leq i \leq N}$ are the eigenvalues of w .

In general results in random matrix theory only become deterministic in the limit $N \rightarrow \infty$. This means that the application of these results to finite size systems has to be conducted carefully and paying special attention to the finite size effects that may arise.

5.1 Infinite systems

Homogeneous network To analyze the homogeneous network model we need to identify the eigenvalue with maximal real part of $-I + \sigma \frac{1}{\sqrt{N}} J$. The spectrum of $\frac{1}{\sqrt{N}} J$ converges to the *circular law*, which was first introduced for matrices whose entries are gaussian random variables in [9] and has been recently generalized to any iid random matrix in [10].

Theorem 5.3 (Circular law). *Let J be any iid random matrix. Then $\mu_{\frac{1}{\sqrt{N}} J}$ converges almost surely to the circular measure μ_c , where $d\mu_c := \frac{1}{\pi} 1_{|z| \leq 1} dz$.*

This means that for $\sigma < 1$ all eigenvalues of the linearized system have negative real part and hence 0 is stable. When σ increases above 1 a continuum of eigenvalues

crosses the imaginary axis. This process is not well understood and does not explain how the transition to chaos takes place.

In general linear stability analysis provides local information and all the other results of this section regard the behavior of the system in the vicinity of 0. However in certain circumstances it is possible to obtain global information using similar techniques. In the appendix C I proof that in the limit $N \rightarrow \infty$ if $\sigma < 1$ then 0 is a globally asymptotically stable fixed point of the homogeneous network model.

Non balanced heterogeneous network When adding the deterministic term of the coupling μM , the balanced and non balanced scenarios have to be analyzed independently because their spectra are qualitatively different. For the case of the non balanced heterogeneous network the following theorem is given in [8]:

Theorem 5.4 (Outliers for small low rank perturbations of iid matrices). *Let J be a $N \times N$ random i.i.d. matrix and let M be a deterministic matrix with rank $O(1)$ and operator norm $O(1)$.*

Let $\epsilon > 0$, and suppose that for all sufficiently large N , there are no eigenvalues of M in the band $\{z \in \mathbb{C} : 1 + \epsilon < |z| < 1 + 3\epsilon\}$, and there are $j = O(1)$ eigenvalues in the region $\{z \in \mathbb{C} : |z| \geq 1 + 3\epsilon\}$.

Then a.s. for sufficiently large N , there are precisely j eigenvalues of $\frac{1}{\sqrt{N}}J + M$ in the region $\{z \in \mathbb{C} : |z| \geq 1 + 2\epsilon\}$ and $\lambda_i(\frac{1}{\sqrt{N}}J + M) = \lambda_i(\frac{1}{\sqrt{N}}J) + O(1)$ as $N \rightarrow \infty$ for each $1 \leq i \leq j$.

In other words there is a finite $\mathcal{O}(1)$ number of eigenvalues of w outside the circle of radius σ . This means that 0 can loose its stability for $\sigma < 1$. In such case, as σ is increased one or more classical bifurcations can take place before the continuum of eigenvalues hits the imaginary axis. After that the dynamics become chaotic.

Balanced heterogeneous network Again in [8] they provide the following result for \bar{J} :

Theorem 5.5. *Let J be an iid random matrix, let $P = (\delta_{ij} - \frac{1}{N})_{1 \leq i, j \leq N}$ so $\bar{J} = JP$ is a balanced iid matrix and let M be a zero row sum matrix. Then $\mu_{\frac{1}{\sqrt{N}}JP+M}$ converges almost surely to the circular measure μ_c .*

This means that the spectrum of w and $\frac{1}{\sqrt{N}}\bar{J}$ converge to the same law and the phase transition is identical to the one of the homogeneous network model. In particular, as the theorem holds for $\mu = 0$, there should be no difference between balanced and non balanced homogeneous network.

5.2 Finite systems

When it comes to finite systems, the spectra are obviously not continuous. This reflects on the transition to chaos. In general most eigenvalues are evenly spread over a circle of radius σ centered at -1.

Homogeneous network Fig. 5a shows the spectrum of $-I + \sigma \frac{1}{\sqrt{N}} J$ for one realization of J with $\sigma = 1$. For σ small enough all eigenvalues have negative real part. For a certain $\sigma \sim 1$ a real eigenvalue (a pair of complex conjugated eigenvalues) crosses the imaginary axis and 0 loses its stability through a Pitchfork (Hopf) bifurcation. As σ is further increased more eigenvalues cross the imaginary axis activating their corresponding modes and eventually leading to chaotic dynamics. This is consistent with the numerical observations and explains the series of bifurcations in Fig. 1.

It is also interesting to know the probability that the first bifurcation is Pitchfork (instead of Hopf) as a function of N or in other words, what is the probability that the eigenvalue with maximal real part is real as a function of N . Fig. 6 shows that as N is increased the probability of having cycles right after the first bifurcation increases. This can be due to the well known fact that the density of eigenvalues of an iid random matrix lying over the real line is $\mathcal{O}(\sqrt{N})$. It is also remarkable that there does not seem to be any difference between J and \bar{J} .

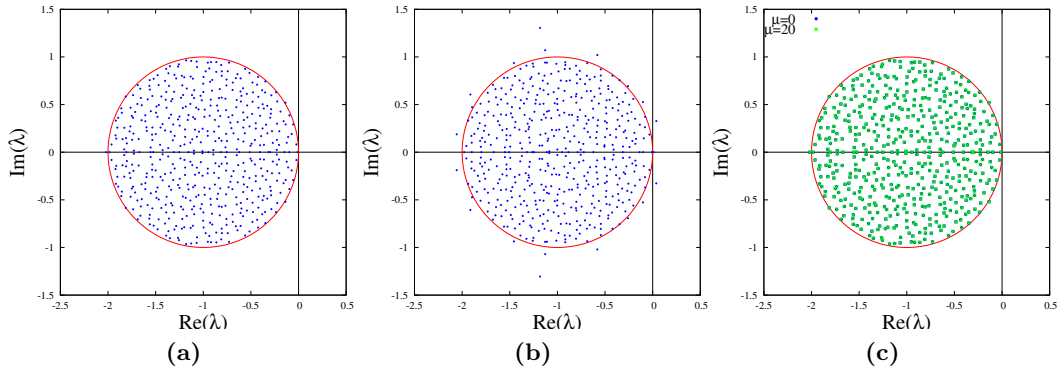


Figure 5: Eigenspectra of $-1 + w$ for a system with $N = 512$ neurons and $\sigma = 1$. (a) $\mu = 0$; (b) $\mu > 0$, J non balanced; (c) superposition of $\mu = 0$ and $\mu > 0$, for the same realization of \bar{J} , both spectra are identical.

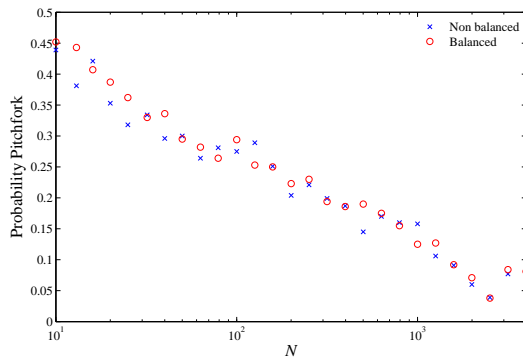


Figure 6: Probability that the eigenvalue with largest real part is real.

Non balanced heterogeneous network Fig. 5b shows the spectrum of a finite size system. The outliers mentioned in theorem 5.4 are also present for finite sizes (in fact their behavior is independent of N). Therefore, before the bulk of the eigenvalues reaches the imaginary axis, the behavior of the finite system is the same as

the one of the $N \rightarrow \infty$ system. After that, as the rest of the eigenvalues cross the imaginary axis, more modes are activated eventually leading to chaos.

Balanced heterogeneous network Fig. 5c shows that the spectra of $-I + \frac{1}{\sqrt{NJ}}$ and $-I + \frac{1}{\sqrt{N\bar{J}}} + \mu M$, not only converge to the same law, but they are identical for finite size systems. Here the linearization around 0 fails to explain the striking differences between the two models.

6 Mean field equations

A rigorous derivation of the mean field equations is in the appendix D. They are

$$\dot{X} = -X + \mu \zeta^{X,Y}, \quad (6.1)$$

$$\dot{Y} = -Y + \sigma \xi^{X,Y} \quad (6.2)$$

where $\zeta^{X,Y}$ and $\xi^{X,Y}$ are gaussian fields centered around 0 with

$$\begin{aligned} \mathbb{E}[\zeta_t^{X,Y} \zeta_{t+\tau}^{X,Y}] &= \text{Cov}[S(X_t + Y_t)S(X_{t+\tau} + Y_{t+\tau})], \\ \mathbb{E}[\xi_t^{X,Y} \xi_{t+\tau}^{X,Y}] &= \begin{cases} \mathbb{E}[S(X_t + Y_t)S(X_{t+\tau} + Y_{t+\tau})] & \text{for non balanced } J \\ \text{Cov}[S(X_t + Y_t)S(X_{t+\tau} + Y_{t+\tau})] & \text{for } \bar{J} \end{cases} \end{aligned}$$

The main difference between the use of J and \bar{J} is that, for reasons similar to those pointed out in section 4, $\text{Cov}[S(X_t + Y_t)S(X_{t+\tau} + Y_{t+\tau})]$ is likely to become small and therefore result in synchronization as opposite to $\mathbb{E}[S(X_t + Y_t)S(X_{t+\tau} + Y_{t+\tau})]$ which is very unlikely to become small.

These mean field equations reproduce the behavior observed numerically and, what is more, setting $\mu = 0$ they are consistent with the equations proposed in [4]. In such case there is no difference between balanced and non balanced couplings because $X = 0$ and since $\mathbb{E}[Y_t] = 0$, then $\text{Cov}[S(Y_t)S(Y_{t+\tau})] = \mathbb{E}[S(Y_t)S(Y_{t+\tau})]$.

7 Conclusions

Based on numerical simulations I provide a description of the behavior of the model under different sets of parameters. I have been able to reproduce the expected results for homogeneous networks and investigate the properties of finite size systems. No difference has been observed between the balanced and non balanced networks. As a side part of the project the probability of observing spontaneous activity in finite homogeneous networks for $\sigma < 1$ has been investigated. Numerical results suggest that there is an optimal system size $N^*(\sigma)$ that maximizes this probability. Numerical observations of the heterogeneous networks reveal new and interesting phenomena that had never been mentioned in previous literature. For the non balanced networks they include qualitatively different bifurcation diagrams and nontrivial mean dynamics. When the coupling is balanced synchronization and relaxation oscillations are the main characteristic features.

Through an heuristic study of the main equations the conditions for having non-trivial mean dynamics and synchronization can be inferred. First setting $\mu > 0$ will result on a non vanishing term in the dynamics of the mean. Second imposing the

balance condition on J will lead to an exponential decay of $\text{Var}[x_i]$ when $\langle x \rangle$ is large. These conditions are consistent with the numerical observations.

Linear stability analysis was performed using multiple results from random matrix theory. The stability of the trivial solution is established for all the scenarios considered. For the homogeneous network linear stability analysis reveals no difference between the balanced and non balanced J . Furthermore, using a new theorem I present here I can proof global asymptotic stability of the trivial solution for $\sigma < 1$ in the limit $N \rightarrow \infty$. For the heterogeneous networks there are critical differences between balanced and non balanced J these differences and their consequences have been analyzed. However linear stability analysis fails to provide an explanation for the new observed phenomena.

Finally I propose a set of mean field equations for the model. I do not proof that these equations are a solution of the original system but I expect to do so in a near future following the proof for the homogeneous model in [6]. After that, stability analysis of the solutions can be performed the same as in [4], specially for the balanced scenario where both gaussian fields have the same covariances.

It will be interesting to generalize these results for not fully connected networks and study the effects of implementing different topologies. It will be also very useful to extend the study of variability to other parameters in order to make the model more biologically plausible.

References

- [1] E. Marder and J.M. Goaillard. Variability, compensation and homeostasis in neuron and network function . *Nature Reviews Neuroscience*, 72, 2006.
- [2] R. May. Will a large complex system be stable? *Nature*, 238, 1972.
- [3] S.I. Amari. Characteristics of random nets of analog neuron-like elements. In *IEEE trans sys man cyber.*, pages 643–657. IEEE Computer Society Press, 1972.
- [4] H. Sompolinsky, A. Crisanti, and H.J. Sommers. Chaos in random neural networks. *Physical Review Letters*, 61(3):259–262, 1988.
- [5] H.J. Sommers, H. Sompolinsky, A. Crisanti, and Y. Stein. Spectrum of large random asymmetric matrices. *Physical Review Letters*, 60(19), 1988.
- [6] G.B. Arous and A. Guionnet. Large deviations for Langevin spin glass dynamics. *Probability Theory and Related Fields*, 102(4):455–509, 1995.
- [7] K. Rajan and L.F. Abbott. Eigenvalue spectra of random matrices for neural networks. *Physical Review Letters*, 97, 2006.
- [8] T. Tao. Outliers in the spectrum of IID matrices with bounded rank perturbations. 2010.
- [9] V.L. Girko. Circular law. 1984.
- [10] T. Tao, V. Vu, and M. Krishnapur. Random matrices: Universality of ESDs and the circular law. *The Annals of Probability*, 38(5):2023–2065, 2010.
- [11] C. Skokos. The Lyapunov Characteristic Exponents and their computation. 2009.

A Numerical simulation details

Numerical simulations were done mostly with CUDA using the algebraic library CUBLAS. The maximal system size efficiently simulated with CUDA was $N \sim 2000$ due to the limited memory of GPUs. Larger systems were simulated using Matlab's Parallel Computing Toolbox reaching $N = 50000$ but involving very long computing times. The integration of the solutions was performed using Runge-Kutta 4 algorithms implemented by myself.

To generate \bar{J} I used the method in [8] which involves projecting an iid random matrix onto the hyperplane $\{(x_1, \dots, x_N) \in \mathbb{C}^n : x_1 + \dots, x_N = 0\}$. In [7] it is said that the balance condition can be relaxed to $\sum_j J_{ij} = \mathcal{O}(1/\sqrt{N})$ still having the same spectral properties. When it comes to the analysis of the trajectories there was not a clear difference between the systems satisfying the original strict balance condition and the ones satisfying the relaxed balance condition. However the later one was avoided because finite size effects became relevant when $\mu \sim \sqrt{N}$ which for the systems I was able to simulate in reasonable computing times was $\mu \sim 40$.

B Optimal system size for spontaneous activity

The spontaneous activity observed in certain neural networks has been subject of recent experimental and theoretical research. To determine if a network is activated or not I compute the maximal Lyapunov exponent λ of the system's attractors. Depending on the value of λ one can distinguish three cases:

- $\lambda < 0$: the attractor is a fixed point, the network is not activated.
- $\lambda = 0$: the attractor is a limit cycle, the network is activated and exhibits regular activity.
- $\lambda > 0$: the attractor is chaotic, the network is activated and exhibits irregular activity.

In terms of λ , we have to estimate $\mathbb{P}[\lambda \geq 0]$.

Due to finite size effects there seems to be an optimal size $N^*(\sigma)$ that maximizes $\mathbb{P}[\lambda \geq 0]$. Furthermore, as σ approaches 1 both the N that maximizes $\mathbb{P}[\lambda \geq 0]$ and the probability itself increase. In the limit case $\sigma = 1$ we do not observe a maximum since $\mathbb{P}[\lambda \geq 0]$ tends asymptotically to 1 (see Fig. 7a). The marginal probabilities corresponding to limit cycles ($\lambda = 0$) and chaotic oscillations ($\lambda > 0$) have a similar behavior. The main difference is that the maximums for $\mathbb{P}[\lambda > 0]$ are reached at larger values of N than the ones for $\mathbb{P}[\lambda = 0]$. As shown in Fig. 7b, this difference means that the larger the system is, the more likely is that the spontaneous activity takes the form of chaotic attractors.

The physical intuitive idea is that as the network grows bigger there is a competition between two opposite phenomena. On the one hand the increasing dimensionality of the system makes it more likely to observe complex behaviors. On the other hand, selfaveraging principles drive the system towards the mean field behavior which for $\sigma < 1$ is the trivial zero solution.

In the numerical simulations λ is computed using the variational equations as shown in [11]. For each matrix size and each value of $\sigma \leq 1$ I analyzed 40000 realizations of the random matrix. For each realization of the connectivity matrix we evolve

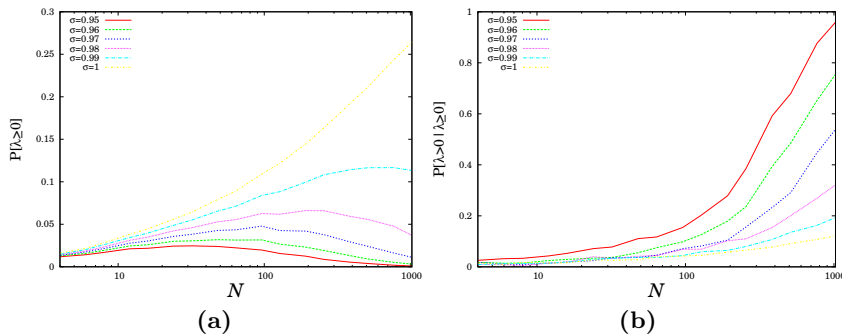


Figure 7: (a) Numerical estimation of the probability of observing spontaneous activity as a function of N and for different values of $\sigma \in \{0.95, 0.96, 0.97, 0.98, 0.99, 1\}$. (b) Probability that the spontaneous activity is chaotic given that there is spontaneous activity.

one solution until it stabilizes and compute an estimation of the Lyapunov maximal exponent $\bar{\lambda}$. The computations are not exact because of the finite sampling time and truncation error so we have some numerical error $\epsilon = \lambda - \bar{\lambda}$. In general the error is small compared to $\bar{\lambda}$. As we are only interested in the sign of λ the error is irrelevant when $\bar{\lambda}$ is clearly positive or negative. However for $\lambda \approx 0$ ϵ becomes relevant to the analysis. In order to overcome this difficulty we fix $\lambda = 0$ when the trajectories are periodic.

C Proof of the global asymptotic stability of 0 for $\sigma < 1$ in the homogeneous network in the limit $N \rightarrow \infty$

I use a contracting argument to proof the global asymptotic stability of 0 for $\sigma < 1$ in the homogeneous network. Linearization of (2.2) at an arbitrary point of the phase space x yields

$$\dot{x}_i = -x_i + \sum_j J_{ij} S'(x_j) . \quad (\text{C.1})$$

To know the local properties of this equation at any point in the space one needs to know the spectrum of a random matrix whose columns have different variances. In particular, for this problem the jacobian is $-I + \frac{1}{\sqrt{N}} JD$ where D is a diagonal matrix whose elements are $d_i = S'(x_i)$ so JD is a matrix where the entries of the j th column have 0 mean and variance $S'(x_j)$. Since $S'(x)$ is bounded by 1 all variances are equal or smaller than one. If under that conditions all eigenvalues have negative real part, the whole phase space is contracting and there can be only one fixed point which is globally asymptotically stable.

To proof that this is the case I provide the following theorem

Theorem C.1. *Let D be a diagonal matrix with elements $\{d_i\}_{i=1, \dots, N}$, then*

$$\rho(JD) \rightarrow \sqrt{\frac{1}{N} \sum_i d_i^2} ,$$

where $\rho(JD)$ is the spectral radius of JD .

Proof. The proof follows the computations of [7] up to equation (7). After that I generalize for N different variances $\{d_i\}_{i=1,\dots,N}$ instead of two obtaining the system

$$0 = \frac{1 + \frac{|\omega|^2}{d_i^2}}{1 + \sum_j r_j} - \frac{|\omega|^2 \sum_j \frac{r_j}{d_j^2}}{(1 + \sum_j r_j)^2} - \frac{1}{Nr_i} . \quad (\text{C.2})$$

Setting $r_i = r_1 q_i$ and comparing the terms of (C.2) that are not common to all equations one gets

$$\frac{|\omega|^2}{d_1^2(1 + \sum_j r_j)} - \frac{1}{Nr_1} = \frac{|\omega|^2}{d_i^2(1 + \sum_j r_j)} - \frac{1}{Nr_1 q_i} \quad (\text{C.3})$$

which implies $q_i = d_i^2$. Hence one has $\sum_j r_j = r_1 \sum_j d_j^2$ □

Using the theorem it is clear that the whole spectrum of $-I + \frac{1}{\sqrt{N}}JD$ lies within a circle of radius $\rho(JD) = \sqrt{\frac{1}{N} \sum_i S'(x_i)^2}$ centered at -1 and therefore for $\sigma < 1$ the whole phase space is contracting.

D Derivation of the mean field equations

I will use the notation defined in (4.1). They mean field equations are obtained taking the $N \rightarrow \infty$ limit of eqs. (2.2) and (2.3) and assuming propagation of chaos. The gaussian fields $\mu\zeta^{X,Y}$ and $\sigma\xi^{X,Y}$ are the $N \rightarrow \infty$ limits of A and B_i assuming that propagation of chaos holds (i.e. in the limit all trajectories are independent stochastic processes given by the same law).

Let's first remark that as J_{ij} are iid random variables with finite variance. By the central limit theorem $\langle J_{ij} \rangle$ will converge to a gaussian random variable with variance $1/\sqrt{N}$. Assuming that in the limit the correlations between different neurons vanish then $\frac{1}{\sqrt{N}} \sum_j \langle J_{ij} \rangle S(x_i)$ is an infinite sum of independent gaussian variables with mean 0 and variance $S(x_i)/N$ and it converges to a gaussian with variance $\mathcal{O}(1/\sqrt{N})$. Since the variance tends to 0 as the system size is increased, this term vanishes when $N \rightarrow \infty$ and can be neglected.

A similar analysis can be performed for J_{ij}

$$\mathbb{E} \left[\lim_{N \rightarrow \infty} \frac{\sigma}{\sqrt{N}} \sum_j J_{ij} S(x_j) \right] = 0 . \quad (\text{D.1})$$

The main difference is that in this case the variance is $\mathcal{O}(1)$ so this term will not vanish and should not be neglected. For A , as M is balanced one can always choose to write

$$\frac{\mu}{\sqrt{N}} \sum_j M_j S(x_j) = \frac{\mu}{\sqrt{N}} \sum_j M_j (S(x_j) - \mathbb{E}[S(x)]) \quad (\text{D.2})$$

and this has obviously expectation 0. Putting these last results together one has

$$\mathbb{E} [\zeta^{X,Y}] = \mathbb{E} \left[\lim_{N \rightarrow \infty} A \right] = 0 , \quad (\text{D.3})$$

$$\mathbb{E} [\xi^{X,Y}] = \mathbb{E} \left[\lim_{N \rightarrow \infty} B \right] = 0 . \quad (\text{D.4})$$

The next step is to find the covariances of $\zeta^{X,Y}$ and $\xi^{X,Y}$. Using again the balance properties of M_j , the fact that $N_E \frac{1-f}{f} + N_I \frac{f}{1-f} = 1$ and statistical independence of every pair of neurons we have

$$\begin{aligned}
\mathbb{E}[\zeta_t^{X,Y} \zeta_{t+\tau}^{X,Y}] &= \mathbb{E} \left[\lim_{N \rightarrow \infty} A_t A_{t+\tau} \right] \\
&= \mathbb{E} \left[\lim_{N \rightarrow \infty} \frac{\mu^2}{N} \sum_j M_j (S(x_j)_t - \mathbb{E}[S(x)]_t) \sum_k M_k (S(x_k)_{t+\tau} - \mathbb{E}[S(x)]_{t+\tau}) \right] \\
&= \mathbb{E} \left[\lim_{N \rightarrow \infty} \frac{\mu^2}{N} \sum_j M_j^2 (S(x_j)_t - \mathbb{E}[S(x)]_t) (S(x_j)_{t+\tau} - \mathbb{E}[S(x)]_{t+\tau}) \right] \\
&= \mu^2 \text{Cov}[S(x)_t S(x)_{t+\tau}] \tag{D.5}
\end{aligned}$$

and similarly for \bar{B}_i

$$\begin{aligned}
\mathbb{E}[\xi_t^{X,Y} \xi_{t+\tau}^{X,Y}] &= \mathbb{E} \left[\lim_{N \rightarrow \infty} (\bar{B}_i)_t (\bar{B}_i)_{t+\tau} \right] \\
&= \mathbb{E} \left[\lim_{N \rightarrow \infty} \frac{\sigma^2}{N} \sum_j J_{ij} (S(x_j)_t - \mathbb{E}[S(x)]_t) \sum_k J_{ik} (S(x_k)_{t+\tau} - \mathbb{E}[S(x)]_{t+\tau}) \right] \\
&= \mathbb{E} \left[\lim_{N \rightarrow \infty} \frac{\sigma^2}{N} \sum_j J_{ij}^2 (S(x_j)_t - \mathbb{E}[S(x)]_t) (S(x_j)_{t+\tau} - \mathbb{E}[S(x)]_{t+\tau}) \right] \\
&= \sigma^2 \text{Cov}[S(x)_t S(x)_{t+\tau}] . \tag{D.6}
\end{aligned}$$

However if J is not balanced one can not subtract the expected value and hence one simply has

$$\begin{aligned}
\mathbb{E}[\xi_t^{X,Y} \xi_{t+\tau}^{X,Y}] &= \mathbb{E} \left[\lim_{N \rightarrow \infty} (B_i)_t (B_i)_{t+\tau} \right] \\
&= \mathbb{E} \left[\lim_{N \rightarrow \infty} \frac{\sigma^2}{N} \sum_j J_{ij} S(x_j)_t \sum_k J_{ik} S(x_k)_{t+\tau} \right] \\
&= \mathbb{E} \left[\lim_{N \rightarrow \infty} \frac{\sigma^2}{N} \sum_j J_{ij}^2 S(x_j)_t S(x_j)_{t+\tau} \right] \\
&= \sigma^2 \mathbb{E}[S(x)_t S(x)_{t+\tau}] , \tag{D.7}
\end{aligned}$$